

broaching, broach, FEM, ABAQUS, alloy EN-AW 6061-T6

Stanisław BŁAWUCKI*, Kazimierz ZALESKI**

CONSTRUCTION AND TECHNOLOGICAL ANALYSIS OF THE BROACH BLADE SHAPE USING THE FINITE ELEMENT METHOD

Abstract

The paper presents results of numerical FEM analyses of the process of broaching the groove using the Explicit module of the ABAQUS program. The impact of the blade geometry was presented and of the selected technological parameters of processing when cutting the aluminium EN-AW 6061-T6 alloy on the load of the broach blade during its operation. This article shows influence of value of rake and clearance angle onto deformations of the tool's cutting edge in the transverse direction. An interaction between broach blade shape and reduced stress in the area of cutting edge was presented. The optimum geometry of the cutting tool was proposed.

1. INTRODUCTION

Broaching is a method of the loss shaping of machine parts. This treatment involves the removal of the material layer with next blades, which are arranged in series. The broach blades, wedge-shaped, perform the rectilinear motion and delving into the treated material they cause its separation. This way, the object gets the final desired shape and dimensions. Broaching is used especially when the processing of parts with other methods is difficult.

In the works, which were created in the 60s of the XX century (Górski, 1967; Monday, 1960), a technology was described, tools and machines used for broaching. In the following years, studies were created on the optimisation of the broaching process (Belov & Ivanov, 1975; Kokmeyer, 1984). Scientific works

* Politechnika Lubelska, Nadbystrzycka 36, 20-618 Lublin, 514 849 284, s.blawucki@pollub.pl

** Politechnika Lubelska, Nadbystrzycka 36, 20-618 Lublin, 81 5384238, k.zaleski@pollub.pl

using the finite element method for the analysis of the broaching were created during the last two decades, with the development of the numerical computational methods. Subsequent citation: Sajeev, Vijaraghavan & Rao (2000) in their research performed the analysis of stress caused in the tool and the workpiece during the simulated cutting of the single broach blade. The cutting model was brought to the issue of free cutting process, also called orthogonal cutting, where the width of the tool blade is greater than the width of the cut layer of the processed object. The works (Schulze, Zanger & Boev, 2013; Xiangwei, Bin, Zhibo & Wenran, 2011; Zhang, Outeiro & Mabrouki, 2015) dealt with the impact of the workpiece's geometry on the dimension and location of the shear plane and on the components of the cutting forces during orthogonal machining. A simplified model was adopted for numerical calculations, in which the width of the tool was equal to the width of the workpiece.

One can encounter many publications from recent years (Kokturk & Budak, 2004; Vogtel, Klocke, Lung & Terzi, 2015) on the optimisation of the blade shape of the broach, based on the strength calculations. However, the strength calculations require knowledge of analytical methods and they assume some safety factors, which leads to the increased size and weight of the tool, as well as deterioration of the technology of the execution of the broach blade.

In the present work, the issue of geometry optimisation of the broach blade to splineways was undertaken, when the criteria included the improvement of performance technology and the reduction of dimensions of the blade cross-sectional area at its basis, in order to shorten the working part of the broach. Decision variables in the computing task include the angles γ and δ , which control the dimensions of the cross-section of the working part. The size of the cross-section of the broach blade at the base affects the value of maximum reduced stress in arrears. The model of orthogonal constrained cutting was used.

2. RESEARCH METHODOLOGY

2.1. Workpiece and tool geometry

The research was carried out on numerical models using the finite element method in the Explicit module of the ABAQUS program. The dimensions of the workpiece and tool were adopted as in figure 1. The scope of the analysed angles of the broach blade was presented in table 1. The reference geometry (d) was selected based on literature recommendations by Górski (1967). The material of the workpiece was chosen for the research – aluminium EN-AW 6061-T6 alloy and the tool material – tungsten carbide (WC) with characteristics given in table 2.

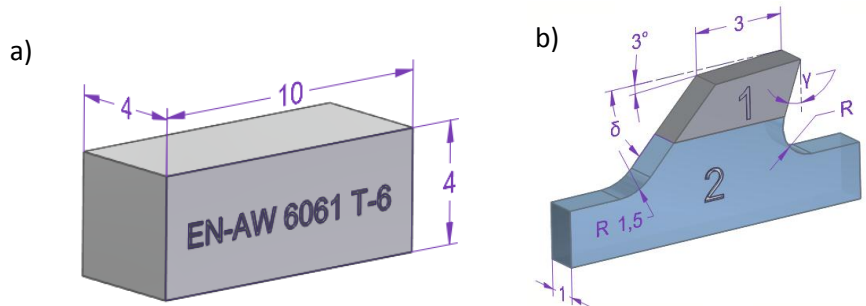


Fig. 1. Characteristic dimensions: a) of the workpiece, b) of the tool: 1 – broach blade, 2 – working part of the broach (excluding the blade) with the chip space

Tab. 1. The values of angles γ and δ of the broach blade defined during numerical analyses

Angle	Values of angles								
γ	0°			10°			20°		
δ	45°	60°	90°	45°	60°	90°	4°	60°	9°
Symbol	a	b	c	d (reference)	e	f	g	h	i

Figure 2a presents the way of restraining the tool and the workpiece. The movement of the workpiece was limited in three directions. The movement of the tool was limited in two directions, a possibility of blade movement was only kept in the parallel direction to the work plane and perpendicular to the cutting edge. A constant thickness of the cutting layer was assumed at 0,25 mm and a constant cutting speed at the level of 50 m/min. The width of the cutting edge results from the length of the cutting edge of the tool and is 1 mm.

Geometrical models of the tool and the work piece (fig. 2b) were divided into finite cubic elements of the C3D8R type with eight nodes and with the side dimension of 0,1 mm. Additionally, at the depth of 0,5 mm from the surface a local density was performed for the mesh in the machined layer of the workpiece to the side dimension of 0,01 mm.

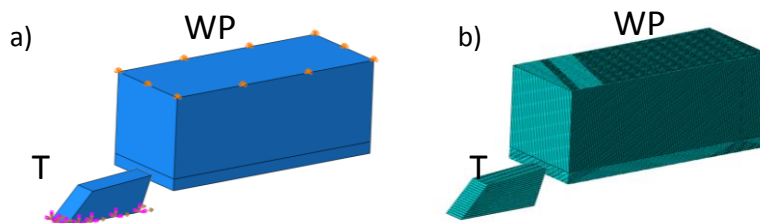


Fig. 2. The system of the workpiece (WP) – tool (T): a) restraint, b) finite element mesh

2.2. Model of the material

With numerical calculations of the cutting process, the constitutive model of the material of Johnson-Cook was implemented (Boldyrev, Shchurov & Nikonov, 2016; Grzesik, 2010; Kosmol & Mieszczyk, 2009; Zhang, Outeiro & Mabrouki, 2015) due to very large plastic deformations in the area of chip formation. The equations for the material takes the form:

$$\bar{\sigma} = \left[A + B \cdot (\bar{\epsilon})^n \right] \cdot \left[1 + C \cdot \ln \left(\frac{\dot{\bar{\epsilon}}}{\dot{\bar{\epsilon}}_0} \right) \right] \cdot \left[1 - \left(\frac{T - T_0}{T_{melt} - T_0} \right)^m \right] \quad (1)$$

where: $\bar{\sigma}$ – equivalent plastic stress,
 A – initial yield stress,
 B – hardening modulus,
 $\bar{\epsilon}$ – equivalent plastic strain,
 n – work - hardening exponent,
 C – coefficient dependent on the strain rate,
 \ln – natural logarithm,
 $\dot{\bar{\epsilon}}$ – equivalent plastic strain rate,
 $\dot{\bar{\epsilon}}_0$ – reference equivalent plastic strain rate,
 T – temperature in the cutting zone,
 T_0 – ambient temperature,
 T_{melt} – melting temperature of the workpiece,
 m – thermal softening coefficient.

Tab. 2. Material properties of workpiece and tool (Boldyrev et al., 2016)

Property or material coefficient	Workpiece	Tool
Density [kg/m ³]	2700	15500
Young's modulus [Pa]	7 · 10 ¹⁰	6,5 · 10 ¹¹
Plasticity [Pa]	A=324,1 · 10 ⁶ B=113,8 · 10 ⁶	–
$\dot{\bar{\epsilon}}$ [s ⁻¹]	10 ⁵	
$\dot{\bar{\epsilon}}_0$ [s ⁻¹]	1	–
Poisson's ratio	0,33	0,21
Friction coefficient	0,15	
C	0.002	–
n	0,17	–
T_0 [°C]	25	–
T_{melt} [°C]	580	–
m	1,34	–

The Johnson-Cook model does not define the beginning of the material destruction, hence the need to use the function describing the initiation of destruction, as well as knowledge of parameters describing the failure process is required. The determination of the five parameters (d_1, \dots, d_5) involves a series of experimental fracture tests, varying the stress triaxiality, strain-rate and temperature (Boldyrev, Shchurov & Nikonov, 2016; Grzesik, 2010; Kosmol & Mieszczak, 2009; Zhang, Outeiro & Mabrouki, 2015). Destruction parameters are summarised in table 3, while the ductile fracture model is described by the equation (2) below:

$$\bar{\epsilon}_f = [d_1 + d_2 \cdot \exp(d_3 \cdot \eta)] \cdot \left[1 + d_4 \cdot \ln\left(\frac{\dot{\bar{\epsilon}}}{\dot{\bar{\epsilon}}_0}\right) \right] \cdot \left[1 + d_5 \cdot \left(\frac{T - T_0}{T_{melt} - T_0}\right) \right] \quad (2)$$

where: $\bar{\epsilon}_f$ – equivalent fracture strain,
 d_1, \dots, d_5 – damage parameters
 η – stress triaxiality parameter,
 \ln – natural logarithm,
 $\dot{\bar{\epsilon}}$ – equivalent plastic strain rate,
 $\dot{\bar{\epsilon}}_0$ – reference equivalent plastic strain rate,
 T – temperature in the cutting zone,
 T_0 – ambient temperature,
 T_{melt} – melting temperature of the workpiece.

Tab. 3. Parameter values of the failure process initiation, (Boldyrev et al., 2016)

Parameter	d_1	d_2	d_3	d_4	d_5
Value	-0,77	1,45	-0,47	0	1,6

In numerical calculations the regeneration function of the mesh of the damaged elements was not used, which in the case of the conducted calculations has got aesthetic qualities and does not impact the results of calculations. Moreover, there is a possibility of the destruction analysis when cutting the composite materials. Then, one should apply the material model described by Dębski & Sadowski (2014).

3. DISCUSSION OF THE RESULTS

The applied material model and the destruction model allowed the analysis of deformations and reduced Huber-Mises stress in spatial system, which were obtained on the cutting edge zone and in the cross-section of the blade of the broach. Due to a small value of deformations of the broach blade (fig. 4), their value can be regarded as negligible.

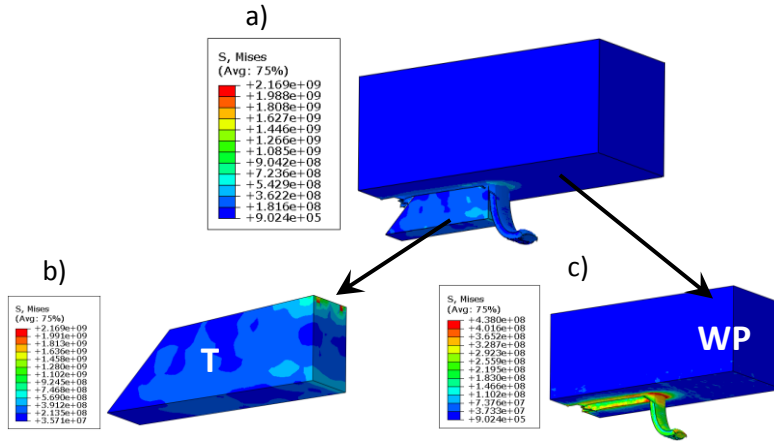


Fig. 3. Examples of the MES analysis results showing the distribution of maximum reduced stresses: a) in the system the workpiece - tool, b) in the tool (T), c) in the workpiece (WP); expressed in Pascals

The reference geometry (d) (fig. 4, 5, 6) of the tool's blade, with the angles of $\gamma = 10^\circ$ and $\delta = 45^\circ$, was characterised by a deformation in the nodes in the zone of the cutting edge at the level of $0,000002$ mm, maximum reduced stress in the tool's cross-section base of $2 \cdot 10^9$ Pa and reduced stress within the cutting edge zone of $8 \cdot 10^9$ Pa.

It was noted that along with the change of angles γ and δ a change of reduced stress took place in the cross-section of the broach blade at the base and in the zone of the cutting edge (fig. 5 and fig. 6). There has been a simultaneous impact of the pair of the studied angles on the value of reduced stress. With the angles $\gamma=0^\circ$ and $\delta=45^\circ$ the maximum reduced stress in the blade's cross-section reaches the lowest value from all analysed cases. With these geometry, the cross-section area of the blade at the base is the largest of the contemplated combinations of pairs of angles.

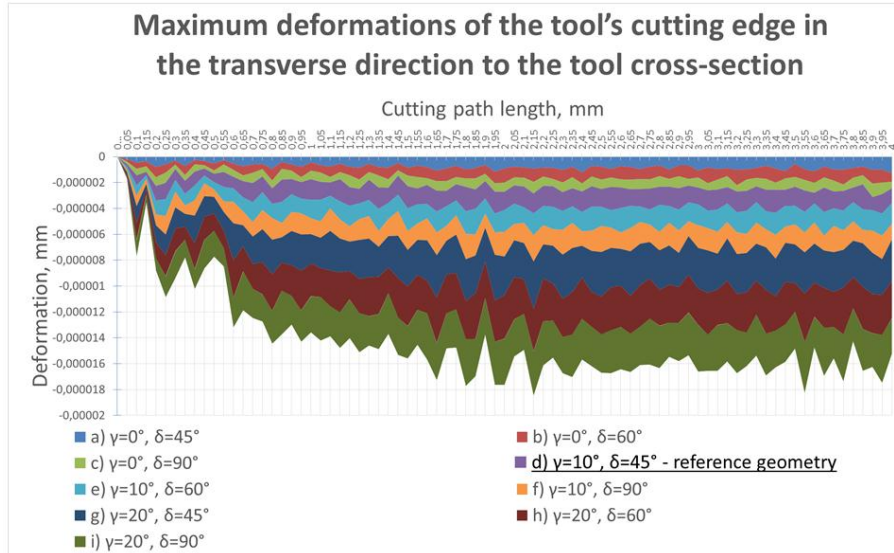


Fig. 4. The curves of maximum deformations of the tool's cutting edge in the transverse direction to the cross-section, in the cutting path function for different angles of the tool's working part

Taking into account the producibility of the performance of the working part of the broach, the best structural solution seems to be the set of blade's angles $\gamma = 0^\circ$ and $\delta = 90^\circ$. This would allow a considerable shortening of the working part of the tool. However, Lipski et al. (2002) says, that with these parameters an adverse build-up edge phenomenon occurs, as well as the rise of temperature on the blade due to the intense chip friction on the tool face. Therefore, one should carry out further explorations of the optimal geometry of the broach blade.

Taking into account the above observations, one can conclude that the optimal solution is a pair of angles of the reference geometry (d). Given that the change of the angle δ from 45° to 90° will increase the stress in the blade's cross-section by 50%, while the producibility of the tool will be improved, and its length will be reduced, this type of compromise is worth noticing, especially for the machining of the aluminium alloy, due to low cutting forces.

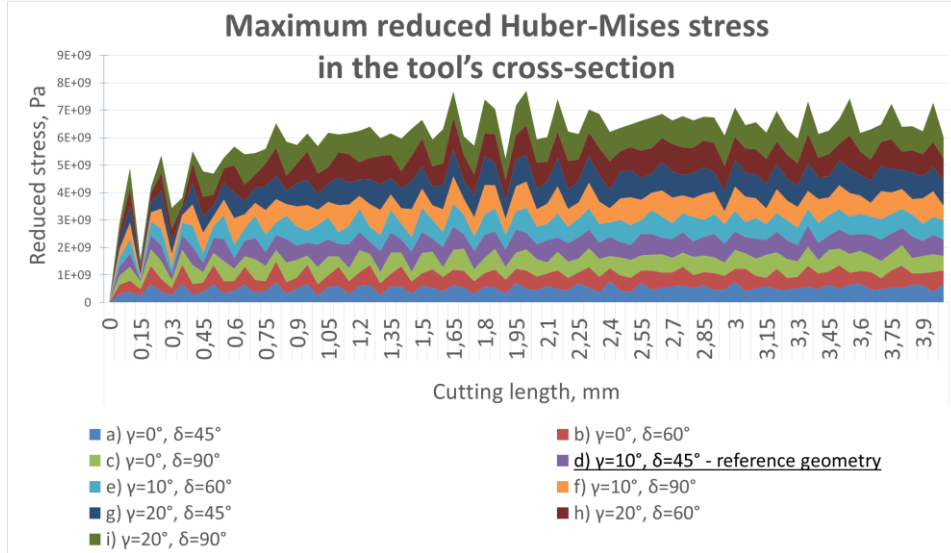


Fig. 5. Curves of the reduced Huber-Mises stress course in the tool's blade cross-section in the function of the cutting length for different angles of the tool's blade

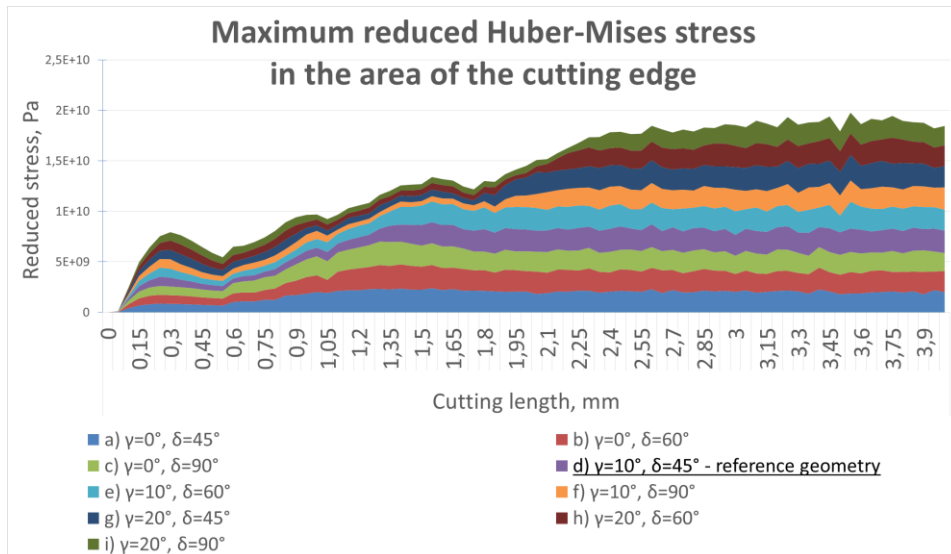


Fig. 6. Curves of the reduced Huber-Mises stress course in the zone of the cutting edge in the function of the cutting path for different angles of the tool's blade

3. CONCLUSIONS

On the basis of numerical analyses and literature review one can draw the following conclusions concerning the analysed geometry of the blade of the broach.

1. Distribution of the deformations and stress in MES models is in line with expectations, as assessed on the basis of gradient maps, obtained for the model of the workpiece and for the tool.
2. According to the assumptions of the numerical analysis, the processed material underwent the plastic deformation of high intensity and elastic deformation, and moreover, there were numerous failure areas of the finite elements and their permanent deformation.
3. The reference geometry (d) of the tool's blade, with the angles $\gamma = 10^\circ$ and $\delta = 45^\circ$ was characterised by a deformation in the cutting edge nodes at the level of 0,000002 mm, maximum reduced stress in the tool's cross-section of $2 \cdot 10^9$ Pa and reduced stress in the zone of the cutting edge of $8 \cdot 10^9$ Pa.
4. Some of the analysed pairs of angles of the working part of the broach exhibit better properties in terms of ultimate strength on the complex condition of stress created in the studied cross-section of the tool during the process of spatial broaching with the carbide blade into the groove of the aluminium EN-AW 6061-T6 alloy.
5. The analysed geometries of the broach's blade (e), (f), (g), (h) and (i) show worse properties in the aspect of ultimate strength to the complex condition of the stress formed in the studied cross-section of the tool during the broaching process.
6. Given the aspect of producibility of the performance of the working part of the broach, the geometry, which $\gamma = 0^\circ$ and $\delta = 90^\circ$, seems optimal, as it allows for a significant reduction of the total length of the broach, by reducing the length of its scale.
7. Reviewing the literature on the subject, the reference geometry, which $\gamma = 10^\circ$ and $\delta = 45^\circ$, is the best solution, taking into account the strength of the tool's blade and the processes occurring in the cutting zone, such as the built-up on the blade.
8. The presented numerical model of broaching the splineways can be of practical use when designing tools and planning of waste machining.

REFERENCE

- Belov, V. S., & Ivanov, G. M. (1975). Improving the accuracy of surface broaching machines. *Stanki i Instrumenty*, 46(7), 6–8.
- Boldyrev, I. S., Shchurov, I. A., & Nikonov, A. V. (2016). Numerical Simulation of the Aluminum 6061-T6 Cutting and the Effect of the Constitutive Material Model and Failure Criteria on Cutting Forces' Prediction. *Procedia Engineering*, 150, 866–870. doi:10.1016/j.proeng.2016.07.031

- Dębski, H., & Sadowski, T. (2014). Modelling of microcracks initiation and evolution along interfaces of the WC/Co composite by the finite element method. *Computational Material Science*, 83, 403–411. doi:10.1016/j.commatsci.2013.11.045
- Górski, E. (1967). *Narzędzia skrawające kształtowe*. Warszawa: WNT.
- Grzesik, W. (2010). *Podstawy skrawania materiałów konstrukcyjnych*. Warszawa: WNT.
- Kokmeyer, E. (1984). *Better Broaching Operations*. Society of Manufacturing Engineers Madison.
- Kokturk, U., & Budak, E. (2004). Optimization of broaching tool design. *Proceedings of the Intelligent Computation in Manufacturing Engineering – 4 Conference, CIRP ICME '04*. Sorrento.
- Kosmol, J., & Mieszczak, W. (2009). Zastosowanie metody elementów skończonych do modelowania procesu wiercenia. *Modelowanie Inżynierskie*, 37, 169–176.
- Lipski, J., Litak, G., Rusinek, R., Szabelski, K., Teter, A., Warmiński, J., & Zaleski, K. (2002). Surface quality of a work material's influence on the vibrations of the cutting process. *Journal of Sound and Vibration*, 252(4), s. 729–737. doi:10.1006/jsvi.2001.3943
- Monday, C. (1960). *Broaching*. London: The Machinery Publishing Co.
- Sajeev, V., Vijaraghavan, L., & Rao, U.R. (2000). An analysis of the effects of burnishing in internal broaching. *International Journal of Mechanical Engineering Education*, 28(2), 163–173.
- Schulze, V., Zanger, F., & Boev, N. (2013). Numerical Investigations on Changes of the Main Shear Plane while Broaching. *Procedia CIRP*, 8, 246–251. doi:10.1016/j.procir.2013.06.097
- Xiangwei, K., Bin, L., Zhibo, J., & Wenran, G. (2011). Broaching Performance of Superalloy GH4169 Based on FEM. *Journal of Materials Science & Technology*, 27(12), 1178–1184. doi:10.1016/S1005-0302(12)60015-2
- Vogtel, P., Klocke, F., Lung, D., & Terzi, S. (2015). Automatic Broaching Tool Design by Technological and Geometrical Optimization. *Procedia CIRP*, 33, 496–501. doi:10.1016/j.procir.2015.06.061
- Zhang, Y., Outeiro, J. C., & Mabrouki, T. (2015). On the selection of Johnson-Cook constitutive model parameters for Ti-6Al-4V using three types of numerical models of orthogonal cutting. *Procedia CIRP*, 31, 112–117. doi:10.1016/j.procir.2015.03.052